Mapping the Valence States of Transition-Metal Elements Using Energy-Filtered Transmission Electron Microscopy

Z. L. Wang,*,† J. Bentley,‡ and N. D. Evans‡

School of Materials Science and Engineering Georgia Institute of Technology, Atlanta, Georgia 30332-0245, and Metals and Ceramics Division, Oak Ridge National Laboratory, Oak Ridge, Tennessee 37831-6376

Received: October 21, 1998; In Final Form: November 23, 1998

The properties of transition-metal oxides are related to the presence of elements with mixed valences, such as Mn and Co. Spatial mapping of the valence-state distribution of transition-metal elements is a challenge to existing microscopy techniques. In this letter, using the valence-state information provided by the white lines observed in electron energy-loss spectroscopy in a transmission electron microscope (TEM), an experimental approach is demonstrated to map the valence-state distributions of Mn and Co using the energy-filtered TEM. An optimum spatial resolution of ∼ 2 nm has been achieved for two-phase Co oxides with sharp boundaries. This provides a new technique for quantifying the valence states of cations in magnetic oxides.

Many physical and chemical properties of inorganic materials are determined by the elements with *mixed valences* in the structural unit,[1] by which we mean that an element has two or more different valences while forming a compound. Transition- and rare-earth-metal elements with mixed valences are unique for initiation of electronic, structural, and/or chemical evolutions. We have demonstrated previously the valence states of Mn and Co in their oxides by applying electron energy-loss spectroscopy (EELS) for quantitative determination.[2−5] In EELS, the L ionization edges of transition-metal, rare-earth, and actinide compounds usually display sharp peaks at the near-edge region. These threshold peaks are known as *white lines*. The unoccupied 3d states form a narrow energy band, the transition of a 2p-state electron to the 3d levels, leading to the formation of white lines observed experimentally. EELS experiments have shown that a change in the valence states of cations introduces significant variation in the intensity ratio of the white lines, giving the possibility of identifying the occupation number of 3d or 4d electrons (or cation valence states) using the measured white line intensities.[6,7]

The information obtained using EELS is an integration over the spatial region illuminated by the incident electron beam. In this paper, we introduce a new experimental approach which can give the distribution maps of cation valences in real space, allowing a direct identification of cations with different valence states. This is useful for studying nanocomposite magnetic oxide materials with mixed valences.

Experimental Section

Figure 1a shows an EELS spectrum of MnO_2 acquired at 200 kV using a Hitachi HF-2000 transmission electron microscope equipped with a Gatan 666 parallel-detection electron energy-loss spectrometer. The oxygen K edge and the Mn L edge are clearly seen. The two sharp peaks are the L_3 and L_2 white lines, the intensity ratio of which is very sensitive to the valance state of Mn. The sharp white lines are the dominant EELS fine structures of transition- and rare-earth-metal elements. EELS analysis of the valence state is carried out in reference to the spectra acquired from standard specimens with known cation valence states. If a series of EELS spectra are acquired from several standard specimens with known valence states, an empirical plot of these data serves as the reference for determining the valence state of the element present in a new compound. Figure 1b shows a plot of the experimentally measured intensity ratios of white lines for Mn. The intensity ratio of L_3/L_2 has little dependence on the specimen thickness, thus no deconvolution is needed for specimens in the most

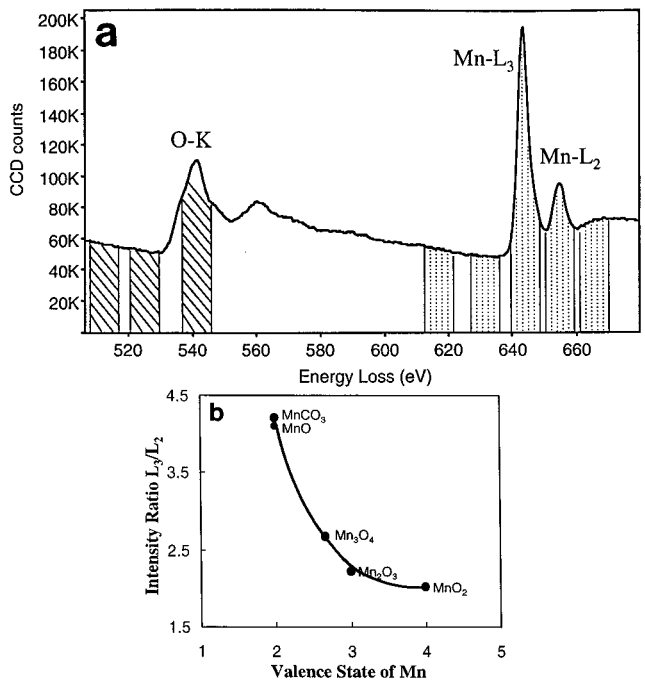

Figure 1. (a) EELS spectrum acquired from MnO_2, showing the technique used to extract the intensities of white lines and the O−K edge. (b) Plot of the intensity ratios of L_3/L_2 calculated from the spectra acquired from Mn compounds as a function of the cation valence. A nominal fit of the experimental data is shown by the solid curve.

† Georgia Institute of Technology.
‡ Oak Ridge National Laboratory.

10.1021/jp9841135 CCC: $18.00
Published on Web 01/15/1999

observable thickness ranges. This is a key point in quantitative mapping of valence states.

In TEM, images formed by electrons with different energy losses can be formed, which is known as the energy-filtered TEM (EF-TEM). We have previously introduced this technique for mapping the distribution of surface-adsorbed organic molecules on Ag nanocrystal surfaces.[8] The information provided by EF-TEM is mostly about the elemental distribution in a thin section of a specimen. To map the distribution of ionization states, an energy window 10 eV in width is required to isolate the L_3 from L_2 white lines. A five-window technique is introduced: two images are acquired at the energy losses prior to the L ionization edges, and they are to be used to subtract the background for the characteristic L-edge signals; two images are acquired from the L_3 and L_2 white lines, respectively; and the fifth image is recorded using the electrons right after the L_2 line that will be used to subtract the continuous background underneath the L_3 and L_2 lines. Then, a L_3/L_2 ratio image will be obtained, which reflects the distribution of the valence state across the specimen. It must be pointed out that for most of the thickness range adequate for EELS analysis, the thickness effect has been removed in the L_3/L_2 image. The detailed experimental procedure for performing energy-filtered TEM can be found elsewhere.[9]

To confirm the information provided by the L_3/L_2 images, the specimen composition is determined from the integrated intensities of the O−K and Mn−$L_{2,3}$ ionization edges by[10]

$$\frac{n_{\mathrm{O}}}{n_{\mathrm{Mn}}} = \frac{I_{\mathrm{O}}(\Delta)}{I_{\mathrm{Mn}}(\Delta)} \frac{\sigma_{\mathrm{Mn}}(\Delta)}{\sigma_{\mathrm{O}}(\Delta)} \tag{1}$$

where $I_{\mathrm{O}}(\Delta)$ and $I_{\mathrm{Mn}}(\Delta)$ are the integrated intensities of the O−K and Mn-L edges for an energy window Δ, respectively, above the ionization thresholds; $\sigma_{\mathrm{Mn}}(\Delta)$ and $\sigma_{\mathrm{O}}(\Delta)$ are the integrated ionization cross-sections for the corresponding energy window, and they can be calculated by the SIGMAK and SIGMAL programs in the hydrogen-like atomic model. From the energy-filtered images, the distribution map of the atomic ratio O/Mn can be calculated.

The MnO_2 powders (grain size < 1 μm) was purchased from Aldrich Chemical Co., and they were dispersed in alcohol ultrasonically. The powders were supported by a thin carbon film and a Cu grid for TEM observation. The EF-TEM experiments were performed using a Philips CM30 (300 kV) TEM, equipped with a Gatan image filtering (GIF) system. This TEM provides the high beam current needed for chemical imaging. The energy window width was selected to be 10 eV, and it took 10−30 s (depending on specimen) exposure to acquire a single raw data image with a satisfactory signal-to-noise ratio. It took ca. 2−4.5 min to acquire a complete set of images, and it was important to ensure the least amount of drift of the specimen during data acquisition.

Results

To demonstrate the application of the EF-TEM for mapping valence states of transition-metal elements, a specimen containing phases with different valences is required. In reference to our previous studies of thermal-induced transition-metal oxides,[2] a reduction of MnO_2 was carried out in situ to a temperature of 350 °C, and the resulting reduced phases were a mixture of oxides of Mn with valences of 2+, 3+, and 4+. This is a model system to be used for mapping the valence-state distribution of Mn.

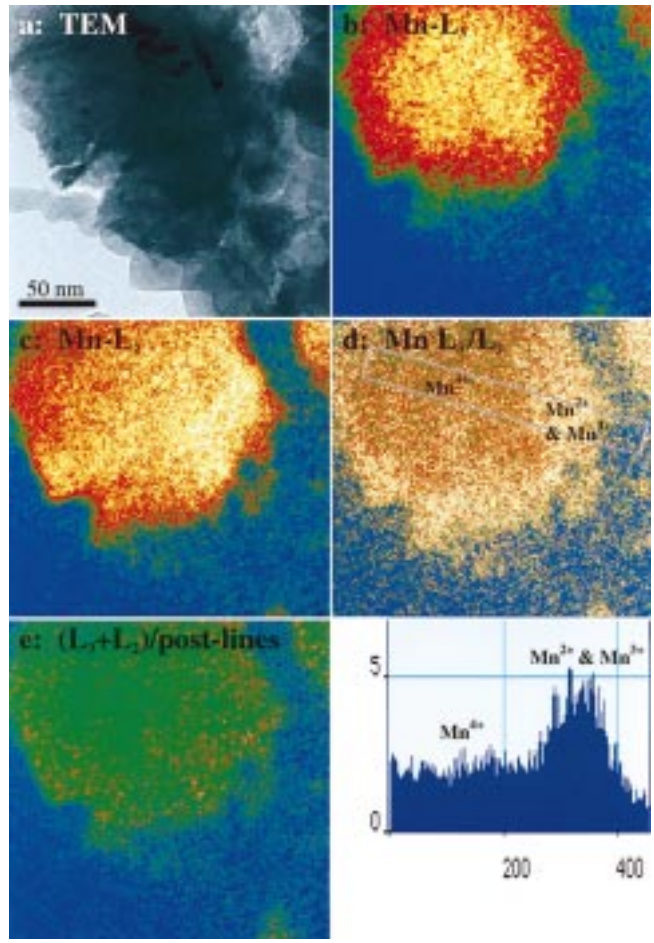

Figure 2. Group of energy-filtered images acquired from the same specimen region of mixed phases of MnO_2 and Mn_3O_4. (a) Conventional bright-field TEM image, (b and c) energy-filtered TEM images of Mn−L_2 and Mn−L_3 white lines, respectively, (d) calculated Mn L_3/L_2 ratio image, and (e) normalized (L_3 + L_2)/post-line image according to the technique of Pearson et al. A pixel-averaged line scan of the L_3/L_2 ratio from (d) is also given, from which the distribution of Mn^{4+}, Mn^{3+}, and Mn^{2+} are identified in reference to the values given by Figure 1b. Each raw image was acquired at 300 kV, an energy window width of Δ = 10 eV for all images except O−K (Δ = 20 eV), and an exposure time of 30 s (at emission current step 1).

Figure 2 shows a series of images acquired by selecting the different energy-loss signals in EELS. From the conventional bright-field image given in Figure 2a, the crystal appears to be a single piece without typical characters. Energy-filtered images using the Mn−L_2 and Mn−L_3 lines (Figures 2b and 2c) show a distinct difference in the intensity distribution. After subtracting the image formed by the continuous energy-loss after the L_2 white line, a ratio image of L_3/L_2 is attained (Figure 2d). A line scan across the image with an average of 50 pixels in width is given below the L_3/L_2 image, from which the distributions of Mn^{4+}, Mn^{2+}, and Mn^{3+} are unambiguously displayed in reference to the white line ratios exhibited in Figure 1b. The reduction of oxides first occurs at the surface region because of the easy desorption of the oxygen, while the core of the crystal is still MnO_2.

On the other hand, a normalized image of (L_3 + L_2)/post line, calculated by dividing the (L_3 + L_2) image by the image acquired using the continuous energy-loss component after (post) the L_2 line, shows no contrast variation across the specimen (Figure 2e). This result proves that the normalization technique introduced by Pearson et al.[6] is less sensitive to the variation of the valence state. Therefore, the L_3/L_2 ratio image is likely

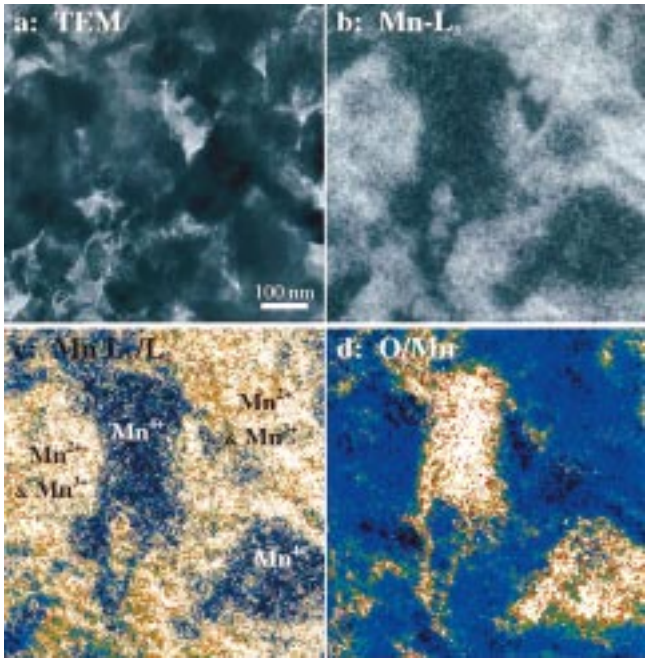

Figure 3. Group of energy-filtered images acquired from the same specimen region of mixed phases of MnO_2 and Mn_3O_4. (a) Conventional bright-field TEM image, (b) energy-filtered TEM images of the Mn−L_3 white line, (c) calculated Mn L_3/L_2 ratio image, and (d) distribution of O/Mn in the region calculated according to eq 1 using the energy-filtered images from the O−K and Mn−L edges. The complimentary contrast of c to d proves the experimental feasibility of valence-state mapping using the white line ratio.

to be the most sensitive technique for mapping the valence distribution.

The major difficulty in EF-TEM imaging is the signal intensity. To demonstrate the attainable spatial image resolution in the valence-state mapping, Figure 3 shows a group of images recorded from an agglomeration of MnO_x with different valences. Again, the bright-field image hardly indicates any information about the valence states of Mn. The EF-TEM Mn−L_3 image reflects the distribution of Mn phases, but its contrast is approximately proportional to the local projected thickness of the specimen. The L_3/L_2 ratio image (Figure 3c) directly gives the distribution of Mn^{4+}, Mn^{2+}, and Mn^{3+}. The low-intensity regions are Mn^{4+}, and the high-intensity regions are the mixed valences of Mn^{2+} and Mn^{3+}, possibly in correspondence to the formation of Mn_3O_4. To confirm this result, the atomic ratio O/Mn image is calculated from the images acquired from the O−K and Mn−L edges, and the result is given in Figure 3d. It is worth pointing out that the O/Mn image is an image of atomic concentrations, independent of specimen thickness. The image clearly indicates that the regions with Mn^{4+} have a higher O atomic concentration because of the balance of the cation charge. This is excellent proof of the information provided by the L_3/L_2 ratio image.

The spatial resolution provided by EF-TEM depends strongly on the quality of the specimen. To give an optimum estimation, a partially oxidized CoO specimen that contains CoO and Co_3O_4 grain structure was chosen.[11] The CoO and Co_3O_4 phases are separated by clear boundaries, and it is an ideal specimen for testing the optimum resolution. Similar EF-TEM experiments have been carried out using the Co−L and O−K edges. The

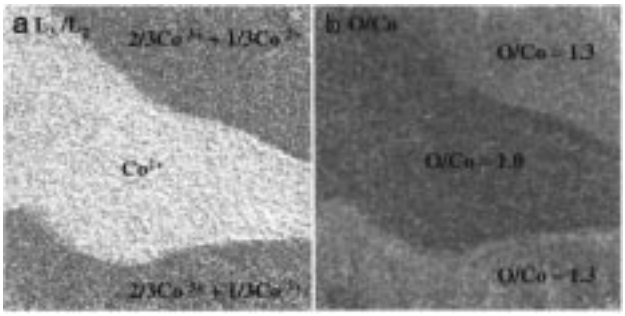

Figure 4. (a) Co L_3/L_2 ratio image recorded from a two-phase CoO and Co_3O_4 specimen, clearly illustrating the distribution of Co valences and the contrast independence of specimen thickness. (b) Distribution of O/Co in the region calculated according to eq 1 using the energy-filtered images from the O−K and Co−L edges for an energy window width of 24 eV. Each raw image was acquired at 300 kV, and energy window width of $\Delta = 12$ eV, and an exposure time of 10 s (at emission current step 3).

valence distribution map is illustrated in Figure 4a, which clearly shows the distribution of Co^{2+} and Co^{3+} in the specimen. The chemical composition ratio image O/Co (Figure 4b) is consistent with the result provided by the valence-state map. A line scan across the valence-state map clearly illustrates that a spatial resolution of 2 nm can be achieved. This is remarkable in comparison to any existing techniques.

In conclusion, a new technique is presented for performing valence-state mapping of transition-metal elements using energy-filtered transmission electron microscopy. This technique gives an optimum spatial resolution of ∼2 nm, and it directly reveals the valence distributions of Mn and Co. This type of information is remarkable for studying the physical chemistry of transition-metal oxides.

Acknowledgment. This research was sponsored by the U.S. NSF, Grant No. DMR-9733160, the Outstanding Overseas Young Scientist Award of China NSF, Grant No. 59825503, the Division of Materials Sciences, U.S. Department of Energy, Contract No. DE-AC05-96OR22464, with Lockheed Martin Energy Research Corp., and the SHaRE Program, contract No. DE-AC05-76OR00033, with Oak Ridge Associated Universities. We thank Drs. A. Revcolevschi, S. McKernan, and C. B. Carter for kindly providing the oxidized CoO specimen.

References and Notes

(1) Wang, Z. L.; Kang, Z. C. *Functional and Smart Materials−Structural Evolution and Structure Analysis*; Plenum Press: New York, 1998.

(2) Wang, Z. L.; Yin, J. S.; Mo, W. D.; Zhang, Z. J. *J. Phys. Chem. B.* **1997**, *101*, 6793.

(3) Wang, Z. L.; Yin, J. S.; Jiang, Y. D. Zhang, J. *Appl. Phys. Lett.* **1997**, *70*, 3362.

(4) Wang, Z. L.; Yin, J. S. *Philos. Mag. B* **1998**, *77*, 49.

(5) Zhang, Z. J.; Wang, Z. L.; Chakoumakos, B. C.; Yin, J. S. *J. Am. Chem. Soc.* **1998**, *120*, 1800.

(6) Pearson, D. H.; Ahn, C. C.; Fultz, B. *Phys. Rev. B* **1993**, *47*, 8471.

(7) Kurata, H.; Colliex, C. *Phys. Rev. B* **1993**, *48*, 2102.

(8) Wang, Z. L.; Harfenist, S. A.; Whetten, R. L.; Bentley, J.; Evans, N. D. *J. Phys. Chem. B* **1998**, *102*, 3068 (and cover).

(9) See *Energy-Filtering Transmission Electron Microsocpy*; Reimer, L., Ed.; Springer Series in Optical Sciences 71; Springer: Berlin, 1995.

(10) Egerton, R. F. *Electron Energy-Loss Spectroscopy in the Electron Microscope*, 2nd ed.; Plenum Press: New York, 1996.

(11) Bentley, J.; McKernan, S.; Carter, C. B.; Revcolevschi, A. *Microbeam Analysis*; Armstrong, J. T., Porter, J. R., Eds.; 1993; Vol. 2 (Suppl.), S286.